Determination of the consumption speed from spherically expanding flame: A new experimental methodology.

Alexandre Lefebvre[1], Hakim Larabi[1], Vincent Moureau[1], Ghislain Lartigue[1], Vincent Modica[1], Emilien Varea[1,*], Bruno Renou[1]

1: CORIA-UMR6614, Normandie Université, CNRS, INSA et Université de Rouen, St Etienne du Rouvray, France

*corresponding author: emilien.varea@coria.fr

Keywords: PIV processing, Laminar burning velocity, Spherically expanding flame

ABSTRACT

Facilities using spherically expanding flame are generally chosen to measure and determine laminar burning velocities. In the 1D planar reference case, laminar burning velocities and consumption speeds are rigorously identical. This is not the case in spherically expanding flames. While the laminar burning velocity is defined from a kinematic point of view, the consumption speed is linked to the integral of the reaction rate across the flame front – kinetic viewpoint. For spherically expanding flame, one of the major question remains in determining the laminar burning velocity from un-biased data or post processing technique. In this work, we propose a new methodology to accurately measure the consumption speed from spherically expanding flame. Theoretical developments expose the way to define the consumption speed for spherically expanding flames. However, the fresh gas density is needed. Therefore, in this work, an optical PIV-based method is developed to determine the fresh gas density profile head of the flame front. Experimental data are provided and compared with DNS data which tend to reproduce the experiment. Good agreement is observed between experimental and numerical data indicating that the methodology exposed in this study is a promising technique to determine the consumption speed from spherically expanding flame experiments.

1. Introduction

Optimization of combustion processes is of major importance to reduce pollutant emissions as well as fuel consumption. Thanks to the emergence of efficient Large Eddy Simulation codes (LES), this is made possible to simulate a full scale combustor such as gas turbine or Internal Combustion Engine (ICE). One of the most important advances remains on the ability of CFD codes to use full chemistry with complex transport. Therefore, accurate data on fundamental

physical flame properties are essential. Laminar burning velocity is an essential quantity which gives information on the mixture's reactivity, diffusivity, and exothermicity. Moreover, laminar burning velocity is one of the very few fuel parameters which can be handled experimentally at relevant conditions for engines or combustor applications.

Among the different techniques, experimental facility using spherically expanding flame is generally chosen as it offers flexibility in terms of initial thermodynamic conditions. Experimental laminar burning velocity data are generally produced and compared to the 1D planar case, which necessitates an extrapolation procedure to zero stretch. For spherical flame configurations, only the propagation speed S_f and the displacement speed relative to the fresh gases $S_{d,u}$ can be measured without any ambiguity[1]. These two quantities might not be representative of consumption speed S_c^f of the flame which is directly linked to the integral of the reaction rate. Fiock and Marvin[2], Linnett[3], Bradley and Mitcheson[4] or and more recently Bonhomme et al.[5] proposed theoretical developments for the consumption speed of the deficient species considering the fresh gas side and assuming constant density for both the burned and fresh gas sides. Note that Lefebvre *et al.*[6] recently developed a generalized expression for the consumption speed of any species for both fresh and burned gas side considerations. They demonstrated that the consumption speed is function of the target species. However, the authors concluded that only the consumption speed written for the deficient species can be used experimentally since it does not require the determination of burned gas parameters as ρ_b or $Y_{k,b}$. These parameters are *a priori* not homogeneously distributed over the burned gas domain and measurements are extremely complicated to achieve with enough accuracy.

The expression of the deficient species consumption speed considering the fresh gas side is

$$S_c^f = S_f - \frac{R_0^3 - R_f^3}{3R_f^2}\frac{1}{\rho_u}\frac{d\rho_u}{dt} = -\frac{1}{\rho_u Y_{k,u} R_f^2}\int_0^{R_0} \dot{\omega}_k\, r^2 dr, \quad (1)$$

where S_f is the propagation speed calculated thanks to the time derivative of the flame radius R_f . R_0 is the internal vessel radius. ρ is the density and subscript u defines the fresh gas side. As previously mentioned, the consumption speed represents the integral of the reaction rate $\dot{\omega}$. Therefore, it is linked to the mass of the deficient species passing through the flame interface. Note that $Y_{k,u}$ is the mass fraction of species k in the fresh gas.

To estimate the consumption speed using **Eq. 1**, the density of fresh gases is mandatory. However, in the recent work of Bonhomme *et al.*[5] the authors developed an another expression of the consumption speeds assuming an isentropic compression for the fresh gases, such as

$$\frac{1}{\rho_u}\frac{d\rho_u}{dt} = \frac{1}{\gamma_u P}\frac{dP}{dt} \quad (2)$$

Therefore, the deficient species consumption speed expression yields

$$S_c^f = S_f - \frac{R_0^3 - R_f^3}{3R_f^2} \frac{1}{\gamma_u P} \frac{dP}{dt} \quad (3)$$

The numerical analysis of Bonhomme *et al.*[5] argued that pressure trace should be easier to measure/determine than that of the density, making the pressure trace P and flame radius evolution $S_f = dR_f/dt$ good candidates for a more precise determination of the consumption speed/burning velocity.

For their work, Andrews and Bradley[7] showed that the values of laminar burning velocity obtained from **Eq. 3** would lead to inaccurate results since this expression is based on the difference of two large numbers. Therefore, only a high fidelity pressure trace measurement might avoid uncertainties when computing the time derivative pressure signal. Consequently, this method is not appropriate for early stages of flame development, when the pressure rise is close to zero (*pre-pressure period*). A sufficient pressure rise is therefore required. Recent studies[1,8,9] have shown that the velocity field ahead of the flame front was accessible using specific tomography algorithms.

From the fresh gas velocity field, we propose in this work to develop expression to access instantaneous fresh gases density while the flame expands, which make possible to evaluate the consumption speed directly.

The objectives of the present work are threefold:

- Develop a theoretical approach for the estimation of the instantaneous density field ahead of the flame front,
- Validate the new approach using 1D DNS methane/air spherically expanding flame simulations,
- Compare the ability of **Eq. 3** and **Eq. 1** to estimate the deficient species consumption speed.

2. Experimental Setup

The apparatus and post-processing methods are described in detailed in[1]. A short description for the optical diagnostic is given below. The tomography technique consists in seeding the mixture with inert silicone oil droplets (Rhodorsil 550) which evaporate in the flame front at $T_{evap} = 570K$. This boiling point temperature is high enough for seeding droplets to penetrating into the preheat zone. The effects of seeding on the flame dynamics, e.g. chemical, sensible enthalpy and re-absorption of radiative energy, have been checked by performing

shadowgraphy measurements with and without seeding droplets in the facility of PRISME's Laboratory in Orléans[10,11]. No significant effects were identified.

The flame front position, $\curlyvee_{tomo}$, is defined at the $570K$ evaporation isotherm of the oil. The magnification ratio is $47\mu m/pxl$ which allows a sufficient definition of the flame front thickness and a good resolution for PIV post-processing tools. In-house PIV post-processing technique enables to resolve the fresh gas velocity profile ahead of the front flame until its maximal value at the entrance of the flame front. This velocity is referred to as $U_{g,u}$. In spherically expanding flame geometry the fresh gas displacement speed is $S_{d,u} = S_f - U_{g,u}$, where S_f is the flame front propagation speed $S_f = dR_{tomo}/dt$.

3. Numerical simulations

In the present work, simulations are conducted with the finite-volume code YALES2[12]. YALES2 is a low-Mach number Large-Eddy Simulation (LES) solver for reactive flows based on unstructured meshes. In this work, YALES2 aims at simulating the experimental setup of Varea *et al.*[1]. The validation of YALES2 code for such configuration is reported in[6]. A brief description is given below.

The simulation domain is a 3D portion of sphere with an opening angle of 0.5 degrees. The radius of the sphere portion evolves between $R_{start} = 2.5mm$ and $R_0 = 82.5mm$. The constructed mesh comports two zones. Between R_{start} and $R = 25mm$, the mesh size is homogeneous and constant at $l = 10\mu m$. This part of the domain corresponds to the area which is experimentally studied. From $R = 25mm$ until R_0, the mesh is growing from $l = 20\mu m\ to\ 200\mu m$. The boundary conditions are periodic on faces tangential to the flame propagation direction and an adiabatic wall is placed at the extremity of the domain to take into account confinement effects. Note that calculations are stopped before the flame front reaches $R = 25mm$. Finite-rate chemistry is setup to provide a realistic description of both thermodynamics of the mixture and transport properties of individual species. The diffusion velocities are obtained using the Hirschfelder and Curtiss approximation[13]. To avoid a drastic time step limitation due to the chemical time scales, a splitting algorithm is implemented in YALES2, which consists in integrating separately the chemistry with a stiff Ordinary Differential Equation solver from the transport and diffusion terms. The flow is considered adiabatic and the flame kernel is ignited by replacing the unburned mixture with burned gases at the same equivalence ratio between $R_{start} = 2.5mm$ and $R_{ignit} = 3mm$. Compared to other strategies with heat deposition for instance, this ignition procedure avoids from fresh gases preheating. All simulations are performed for atmospheric

initial thermodynamic conditions, i.e. a temperature of $T = 300K$ and a pressure of $P = 1atm$. For *CH4/air* flames, simulations were performed with the GRI-mech 3.0 mechanism[14], which counts 53 species and 325 reversible reactions.

3. Theoretical development

In this section, the theoretical development which allows to gives an expression for the instantaneous fresh gas density is described.

The fresh gas density corresponds to the ratio between the fresh gas mass and the volume it occupies. The temporal evolution of this quantity can be estimated on a fixed volume by measuring the flux entering and/or leaving through its edge. This flux is directly linked to the fresh gas velocity, a quantity which can be measured from PIV experiments. However, operate with a fixed volume might be difficult from an experimental point of view to estimate the fresh gas density during the flame propagation. Indeed, the flame front might reach the volume edges if the latter is chosen too close to the ignition point. Moreover, if the control volume is chosen to far from the ignition point the determination of the fresh gas velocity might be difficult since the fresh gases are nearly motionless. Consequently, another type of volume has to be considered. In the present study, we propose to develop the continuity equation in an arbitrary volume $V_a(t)$ adjusted at each time step which allows to estimate the temporal evolution of the unburned density ρ_u .

We define a material control volume $V_m(t)$. The latter moves with the fluid such as the velocity at one point of its bordering surface is equal to the local fluid velocity U. The mass conservation equation without sources or holes is defined such as

$$\frac{d}{dt}\int_{V_m(t)} \rho dV = 0 \tag{4}$$

Following the transport theorem, an arbitrary control volume $V_a(t)$ which coincides with $V_m(t)$ at time *t* but does not necessarily move at the fluid velocity can be introduced such as **Eq. 4** yields

$$\frac{d}{dt}\int_{V_m(t)} \rho dV = \frac{d}{dt}\int_{V_a(t)} \rho dV + \oint_{A_a(t)} \rho(\vec{U} - \dot{\vec{X}}) \cdot \vec{n}\, dA = 0 \tag{5}$$

where $\dot{X}$ is the local velocity of the area $A_a(t)$ bordering the volume $V_a(t)$. U is the fluid velocity at the location X. Using an arbitrary volume is extremely convenient since any boundary surface can be selected. **Figure 1** represents the arbitrary volume considered in the present study. It consists of a spherical volume containing the fresh gases from a radius $R = X$, with X fixed at a constant distance d of the flame front at each time step, to the vessel wall at $R = R_0$.

Integrating **Eq. 5**, projected on the radial axis, between time t^n and t^{n+1} leads to

$$\frac{(\int \rho dV)^{n+1} - (\int \rho dV)^{n}}{t^{n+1} - t^{n}} - \oint_{\Sigma^{n+1/2}} \rho(U - \dot{X})\ dA = 0 \tag{6}$$

Then, assuming

$$\rho^{n+1/2} = \frac{\rho^{n+1} + \rho^{n}}{2} \tag{7}$$

the temporal fresh gas density evolution can be estimated at each time step by

$$\rho_u^{n+1} = \rho_u^{n} \frac{\left[\frac{R_O^3 - (X^n)^3}{3\Delta t} + \frac{1}{2}\left(\frac{X^{n+1} + X^n}{2}\right)^2 (U^{n+\frac{1}{2}} - \frac{X^{n+1} + X^n}{\Delta t})\right]}{\left[\frac{R_O^3 - (X^{n+1})^3}{3\Delta t} - \frac{1}{2}\left(\frac{X^{n+1} + X^n}{2}\right)^2 (U^{n+\frac{1}{2}} - \frac{X^{n+1} + X^n}{\Delta t})\right]} \tag{7}$$

This equation requires the initial fresh gas density ρ_u^0, the position X of the area $A_a(t)$ at each time steps and the fresh gas velocity U through the area $A_a(t)$ between two consecutive time steps. These parameters are experimentally measured following the procedures described in Section 2. Results and validation are presented in the next sections.

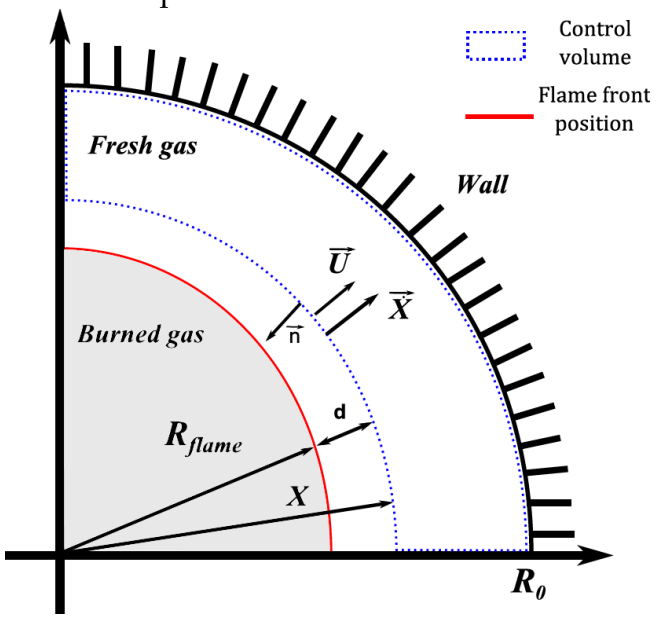

Fig. 1 Scheme of an infinitely thin flame located at $R = R_f$ and the temperature and velocity profiles to represent all parameters needed in the present study.

5. Results

In this section, validations of the experimental procedure as well as the theoretical developments are provided using simulations from YALES2 code on a stoichiometric *CH4/air* flame.

5.1 Validation of the experimental procedure

The precision of S_f and $U_{g,u}$ measurements is reported in **Fig. 2** where numerical and experimental profiles of normalized fresh gas velocity, temperature and fuel mass fraction of a stoichiometric *CH4/air* flame at a temperature of $T = 300K$ and a pressure of $P = 1atm$ are presented. One might observe that the camera spatial resolution is sufficient enough to experimentally determine with accuracy the fresh gas velocity $U_{g,u}$ at R_{U_g} since it is well identified on a non-dispersed profile. Furthermore, based on numerical profiles of temperature and fuel mass fraction, it is observed that the two radii R_f and R_{tomo} are very close to each other. The location of R_{tomo} from calculation is obtained at the isotherm $T = 570K$. Consequently, R_{tomo} seems to be a good candidate to replace R_f in **Eq. 1**.

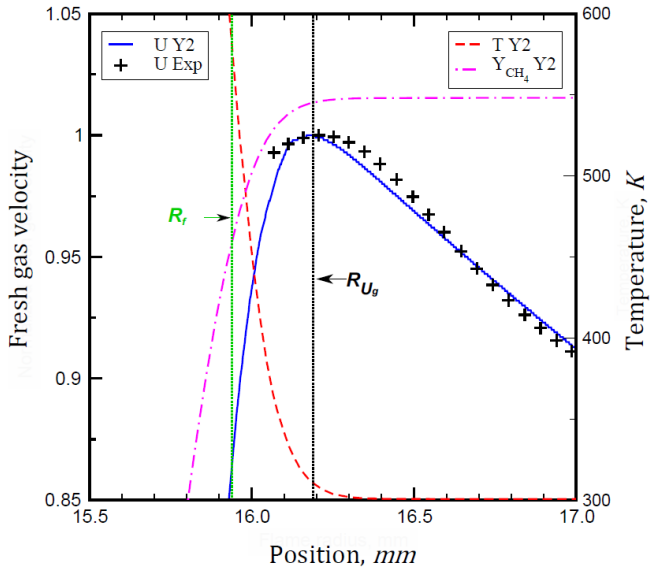

Fig. 2 Numerical and experimental profiles of normalized fresh gas velocity, temperature and fuel mass fraction of a stoichiometric CH4 /*air* flame. $P = 1atm$, $T = 300K$. Y2 stands for simulations from YALES2 code.

5.2 Validation of the experimental procedure

Figure 3(a) shows the evolution as a function of the flame radius of the second Right Hand side (RHS) term of **Eq. 1** which is $\frac{1}{\rho_u}\frac{d\rho_u}{dt}$. For statistical purposes, four experimental tries are considered. Numerical results for the stoichiometric *CH4/air* flame at a temperature of $T = 300K$ and a pressure of $P = 1atm$ are also reported. From **Fig. 3(a)**, repeatability and accuracy of experimental data and post-processing technique on the fresh gas density measurements are demonstrated.

To the author knowledge, it is the first time that an optical technique for instantaneous density measurements on confined spherically expanding flame is proposed. Therefore, the assumption of isentropic compression to overlay the difficulty in measuring the consumption speed is not necessary.

Figure 3(b) shows a comparison between the second RHS term of **Eq. 1** and **Eq. 3**. It clearly appears that even though pressure trace is experimentally recorded using high accuracy sensors, its time derivative function is extremely sensitive which lead to high inaccuracy. It is worth noting that no fitting procedure is applied on the pressure or on the density signals to avoid any biases on the derivative process. Indeed, the pressure elevation is lower than 3% for a flame radius of 2cm considering the *CH4/air* in this experimental configuration. As a consequence, using the pressure trace is not accurate enough to estimate the compression term for this flame development interval.

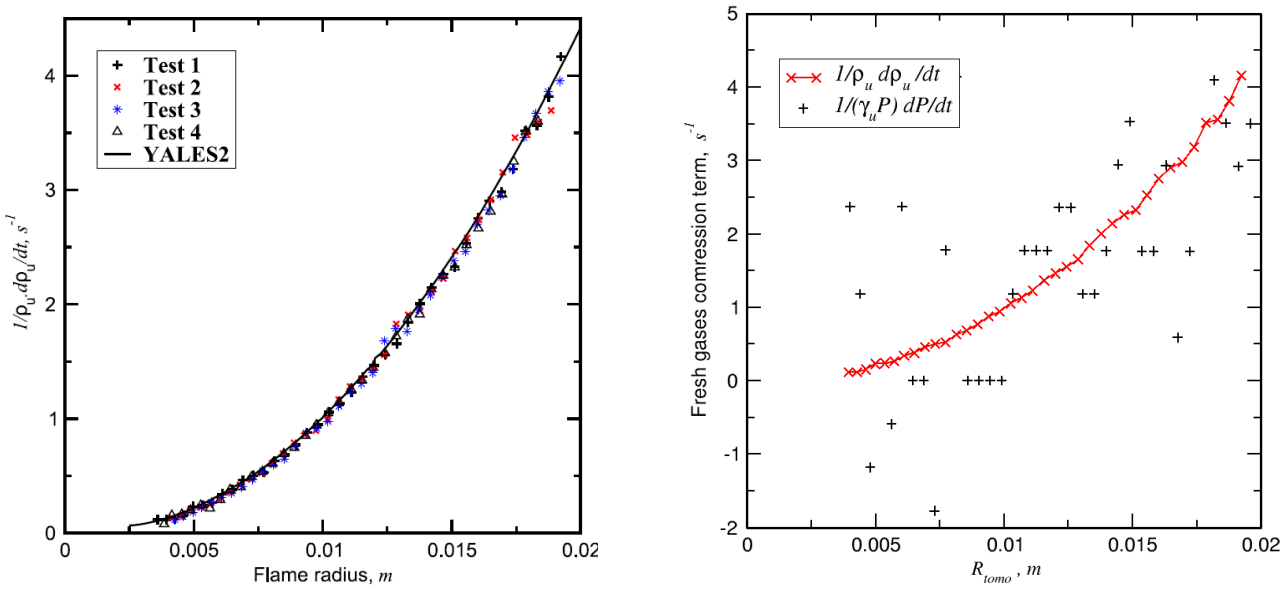

a) **b)**

Fig. 3 Left: Time derivative of the fresh gas density compared to simulation with respect to the experimental flame radius. Right: Comparison between the experimentally determined two terms $\frac{1}{\rho_u}\frac{d\rho_u}{dt}$ and $\frac{1}{\gamma_u P}\frac{dP}{dt}$ with respect to the experimental flame radius. Stoichiometric *CH4/air* flame at $T = 300K$ and $P = 1atm$.

5.1 Consumption speeds for stoichiometric methane air flames

Hereafter, consumption speed over stretch is reported in **Fig. 4** for the stoichiometric *CH4/air* flame at $T = 300K$ and $P = 1atm$. Both experimental (empty symbols) and numerical data (filled symbols) are provided. Dash lines represent linear extrapolation of numerical results. In **Fig. 4**,

the density weighted displacement speed relative to the burnt side $\widetilde{S_{d,b}}$ is also reported. This velocity appears to be the most popular way to estimate the burning velocity. Many assumptions are done to derive $\widetilde{S_{d,b}}$ which in the end yields as easy expression such as $\widetilde{S_{d,b}} = \frac{\rho_b^{eq}}{\rho_u}\frac{dR_f}{dt}$ where ρ_b^{eq} is the burned gas density at the equilibrium conditions. From this expression, it appears that only the flame front propagation speed needs to be recorded from experiments. The densities for both the fresh and burnt sides are evaluated using an equilibrium solver. Therefore it is of major importance to compare the velocity $\widetilde{S_{d,b}}$ with the properly derived consumption speed S_c^f from **Eq. 1**.

We observe that both experimentally and numerically, $\widetilde{S_{d,b}}$ and S_c^f are in very good agreement. Moreover, both velocities gives very similar results over stretch and their sensitivity to stretch (Markstein length) are very similar. This result corroborates the first observation done by Bonhomme *et al.*[5] where the authors assumed isentropic compression for S_c^f. As explained in Bonhomme *et al.*[5], since the *CH4/air* flame exhibits a unity Lewis number, most of the assumptions made to derive $\widetilde{S_{d,b}}$ are validated. However, as soon as off-unity Lewis number flames are concerned, both velocities $\widetilde{S_{d,b}}$ and S_c^f would lead to different values and sensitivity to stretch behavior would not be identical, as mentioned by [15, 16]. As a consequence, it is important to verify whether the consumption speed is well determined when using $\widetilde{S_{d,b}}$ expression.

Therefore, thanks to the theoretical development, advanced optical diagnostics and post-processing algorithms, an opportunity to accurately estimate the consumption speed S_c^f is given.

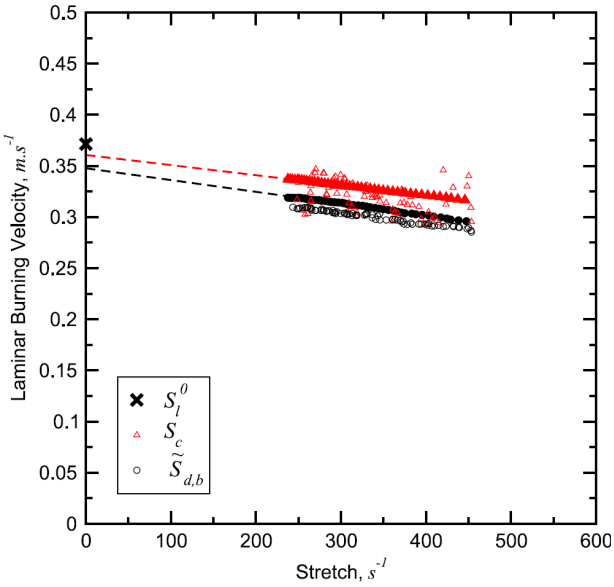

Fig. 4 Comparison between numerical (filled symbols) and experimental (empty symbols) data of consumptions speed definitions of CH4=air flames at atmospheric conditions. The cross at

zero stretch corresponds to the value of the burning velocity obtained from calculation of a planar flame.

6. Conclusion

In this work, a theoretical development to access the fresh gas density in spherically expanding flames configuration is conducted. This makes it possible to determine the consumption speed of various mixtures limiting the assumptions such as isentropic compression or burned gases state.
In parallel, the experimental data are validated using the YALES2 code. An excellent agreement between both experimental data and simulations is shown. Therefore, both the experimental setups as well as the theoretical developments are validated on a stoichiometric methane air flame.
The consumption speed is accessed without ambiguity, which makes this new approach a promising technique to extract accurate data of consumption speed for various fuels.

References

[1] E. Varea, V. Modica, A. Vandel, B. Renou, Measurement of laminar burning velocity and markstein length relative to fresh gases using a new post processing procedure: Application to laminar spherical flames for methane, ethanol and isooctane-air mixtures, Combustion and Flame 159 (2012) 577–590.
[2] E. Fiock, C. Marvin, The measurment of flmae speeds, Chemical Reviews 21 (1937) 367–387.
[3] J. W. Linnett, Six lectures on the basic combustion process. Detroit, Michigan: ETHYL Corporation (1954) 1–37.
[4] D. Bradley, A. Mitcheson, Mathematical solutions for explosions in spherical vessels, Combustion and Flame 26 (1976) 201–217.
[5] A. Bonhomme, L. Selle, T. Poinsot, Curvature and confinement effects for flame speed measurements in laminar spherical and cylindrical flames, Combustion and Flame 160 (7) (2013) 1208–1214.
[6] A. Lefebvre, H. Larabi, V. Moureau, V. Modica, E. Varea, B. Renou, Formalism for spatially averaged consumption speed considering spherically expanding flame configuration, submitted to Combustion and Flame.

[7] G. Andrews, D. Bradley, Determination of burning velocities: A critical review, Combustion and Flame 18 (1972) 133–153.

[8] E. Varea, V. Modica, B. Renou, A. M. Boukhalfa, Pressure effects on laminar burning velocities and mark- stein lengths for isooctane-ethanol-air mixtures, Proceedings of the Combustion Institute 34 (1) (2013) 735–744.

[9] E. Varea, J. Beeckmann, H. Pitsch, Z. Chen, B. Renou, Determination of burning velocities from spheri- cally expanding h2/air flames, Proceedings of the Combustion Institute 35 (2015) 711–719.

[10] T. Tahtouh, F. Halter, C. Mounaim-Rousselle, Measurement of laminar burning speeds and markstein lengths using a novel methodology, Combustion and Flame 156 (2009) 1735–1743.

[11] F. Halter, T. Tahtouh, C. Mounaim-Rousselle, Nonlinear effects of stretch on the flame front propagation, Combustion and Flame 157 (2010) 1825–1832.

[12] TEAM CORIA CFD, http://www.coria-cfd.fr (2015).

[13] T. Poinsot, D. Veynante, Theoretical and Numerical Combustion, Third Edition (www.cerfacs.fr/elearning), 2011.

[14] G. Smith, D. Golden, M. Frenklach, N. Moriarty, B. Eiteneer, M. Goldenberg, C. Bowman, R. Hanson, S. Song, W. G. Jr., V. Lissianski, Z. Qin, Gri-mech homepage, http://www.me.berkeley.edu/gri_mech/.

[15] C. Law, Dynamics of stretched flames, Proceedings of the Combustion Institute 22 (1989) 1381–1402.

[16] P. Clavin, F. Williams, Effects of molecular diffusion and thermal expansion on the structure and dynamics of premixed flames in turbulent flows of large scale and loaw intensity, Journal of Fluid Mechanics 116 (1982) 251 – 282.